Available online at www.sciencedirect.com

ScienceDirect

Coordination Chemistry Reviews 250 (2006) 2595–2609

COORDINATION CHEMISTRY REVIEWS

www.elsevier.com/locate/ccr

Review

Metal complexes of 4,4′-dipyridyldisulfide—structural diversity derived from a twisted ligand with axial chirality

Ryo Horikoshi[a], Tomoyuki Mochida[a,b,*]

[a] Department of Chemistry, Faculty of Science, Toho University, Funabashi, Chiba 274-8510, Japan
[b] Research Center for Materials with Integrated Properties, Faculty of Science, Toho University, Funabashi, Chiba 274-8510, Japan

Received 13 December 2005; accepted 5 April 2006
Available online 18 April 2006

Contents

Abstract

This review describes our recent results and other relevant studies into the preparation and structures of metal complexes with the sulfur-bridged bis-pyridine ligand 4,4′-dipyridyldisulfide (4DPDS). More than 30 structurally characterized 4DPDS complexes of various structural types including macrocycles, zigzags, helices and repeated rhomboids are known. Although 4DPDS is a simple bridging ligand, its twisted structure and axial chirality provide structural diversity as well as guest inclusion properties for the complexes.

Keywords: Self-assembly; Coordination polymer; 4,4′-Dipyridyldisulfide; Supramolecular isomerism

1. Introduction

The design and synthesis of coordination polymer complexes are of considerable interest from the viewpoint of crystal engineering [1–6]. The well-defined infinite network topologies that appear in these solids are attractive to chemists for esthetic reasons [5,7], and various functional materials have been developed based on their guest-inclusion [3–8] and physical properties [6,9,10].

The structural motifs of the coordination polymers range from zero- to three-dimensional, where the term “zero-dimensional” refers to a discrete structure, such as a macrocycle or a molecular square. Because high-dimensional architectures often allow guest inclusion, increasing dimensionality is an important theme in coordination polymer chemistry [3–6,8,11,12]; even some complexes with zero- or one-dimensional structures can enclathrate small molecules [13–15].

The structures and properties of coordination polymers can be controlled by choosing appropriate bridging ligands and metal ions. Many types of bridging ligand have been reported, of which the most extensively studied bidentate ligands are probably 4,4′-bipyridine (4BPY) [4,5,11,12] and its analogs (Fig. 1). Spacer groups can be introduced into 4BPY to produce a variety of linear and bent bridging ligands. 4BPY analogs with linear spacers produce rectangles, linear chains, zigzag chains, grids and lattices (Fig. 2a) when combined with metal salts [3–9,11]. For example,

---

[*] Corresponding author. Tel.: +81 47 472 4406; fax: +81 47 472 4406.
E-mail address: mochida@chem.sci.toho-u.ac.jp (T. Mochida).

0010-8545/$ – see front matter © 2006 Elsevier B.V. All rights reserved.
doi:10.1016/j.ccr.2006.04.002

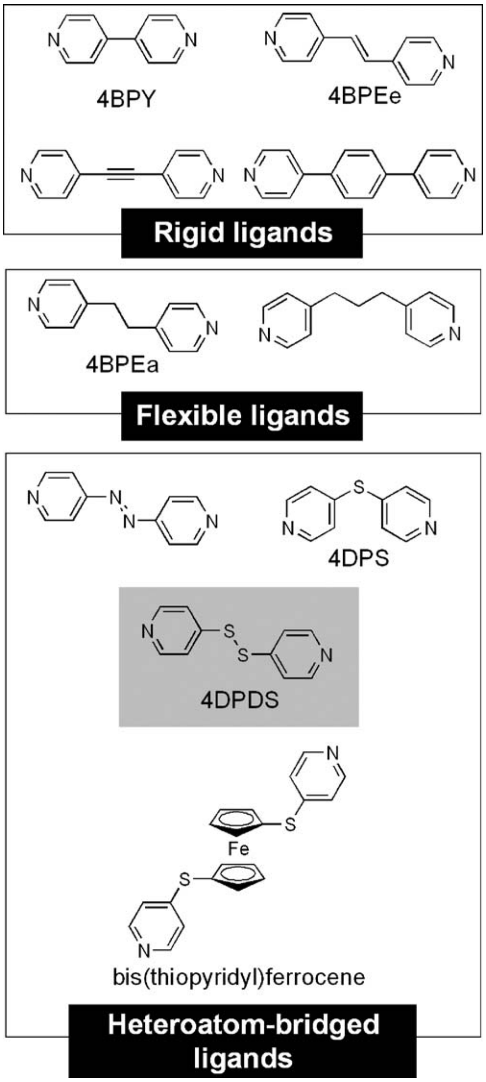

Fig. 1. Examples of 4,4′-bipyridine analogs.

combination of linear ligands containing phenylene and acetylene spacers with *cis*-protected square-planar Pd(II) and Pt(II) ions produces a series of molecular squares [16,17]. Flexibility can be introduced to the ligand by incorporation of alkyl spacers, leading to remarkable changes in the resultant assembled structures. Coordination polymers that contain flexible ligands show zigzag chain, helical chain and repeated rhomboid structures (Fig. 2b) [18–22].

Coordination polymers with bis-pyridine-type ligands carrying heteroatoms have been extensively developed in recent years [23–28]. The introduction of a non-alkyl spacer between the two 4-pyridine groups has a dramatic effect: because chalcogen and amine spacers give the ligand a bent structure, the assembled coordination polymers are structurally more complicated than those that contain linear ligands. Further, the chalcogen and amine moieties have additional coordination ability as well as the ability to accept hydrogen bonds, which may lead to increased dimensionality.

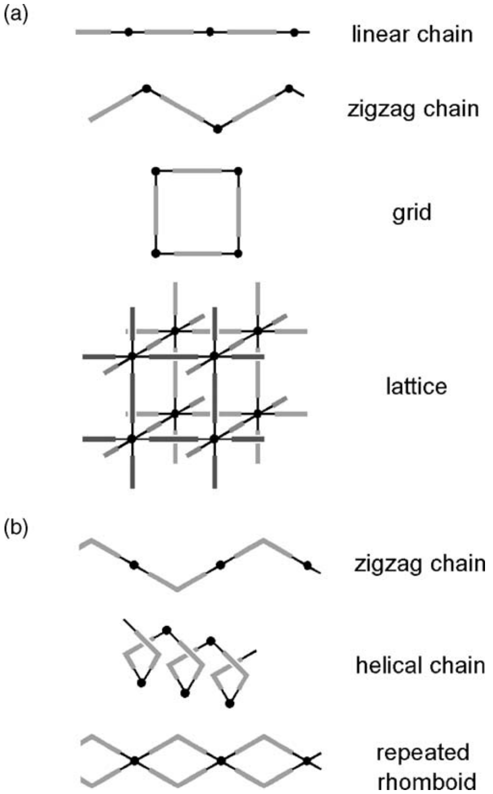

Fig. 2. Schematic illustrations of the structural motifs of metal complexes from 4,4′-bipyridine analogs with (a) linear spacers and (b) flexible spacers.

We have studied complexes of metals with 4,4′-dipyridyldisulfide (4DPDS; Fig. 1), which has a characteristic twisted shape. This review covers the synthesis and structures of 4DPDS complexes, arranged according to their dimensionality (zero-, one- and two-dimension). To the best of our knowledge, three-dimensional coordination polymers with 4DPDS have not been reported. In particular, we highlight the correlation of the overall structures of 4DPDS complexes with the coordination geometries of the metal ions and the shapes of the counter anions. Further, we describe the supramolecular isomerism phenomenon [4] observed for 4DPDS coordination polymers.

More than 30 complexes of 4DPDS with transition-metal species, such as Mn(II), Fe(II), Co(II), Ni(II), Cu(I), Cu(II), Zn(II), Ag(I), Cd(II), Ir(III) and Pt(II) are known. The importance of selecting an appropriate metal ion for rational design has been well documented [3–7,29]. The structural diversity of 4DPDS coordination polymers is mainly a result of the ligand's characteristic twisted structure, but is also correlated with the coordination geometry of the metal ions (Fig. 3).

2. Characteristic features of 4,4′-dipyridyldisulfide

4DPDS shows a characteristic twisted structure, with a C–S–S–C torsion angle of approximately 90°. This ligand has axial chirality, which generates *M*- and *P*-enantiomers as shown in Fig. 4. The disulfide moiety is relatively rigid and maintains its characteristic torsion even when coordinated to metal ions in the solid state. Metal complexes with 4DPDS are interesting in terms of chiral crystal engineering, although chiral crystals containing the ligand have not yet been produced. A characteristic feature of the ligand is the easy cleavage of the S–S bond. Asym-

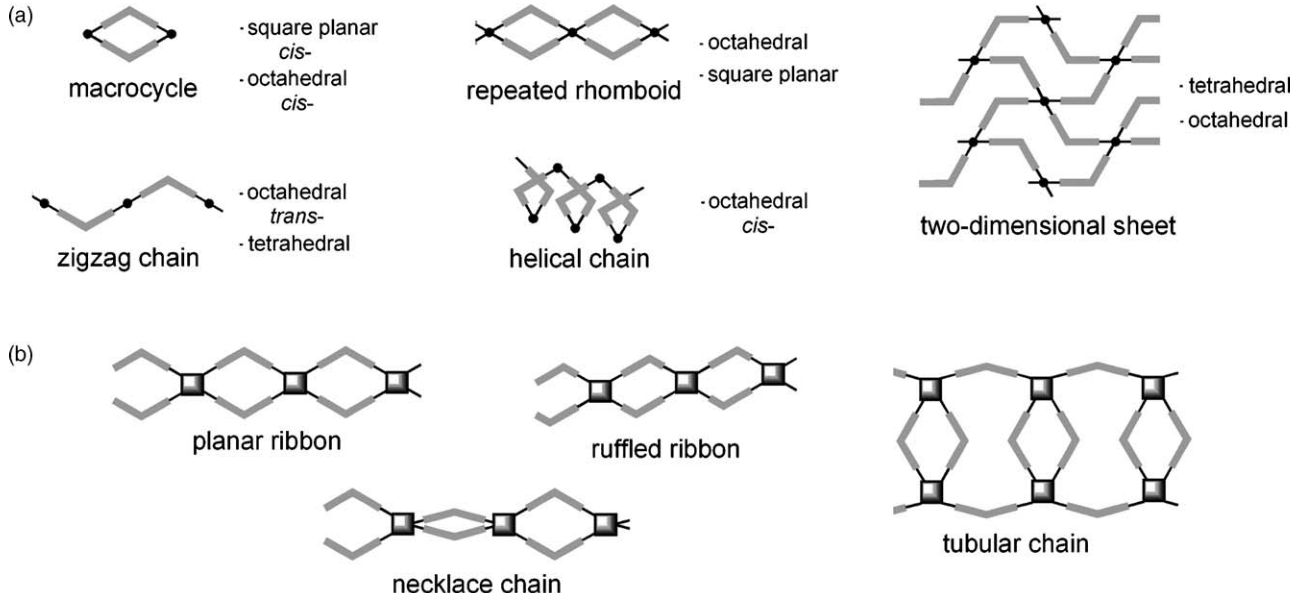

Fig. 3. (a) Schematic illustration of the assembled structures of 4DPDS complexes. Correlation between structural topology and metal coordination geometries are shown. (b) Schematic illustration of 4DPDS complexes involving multinuclear metal units.

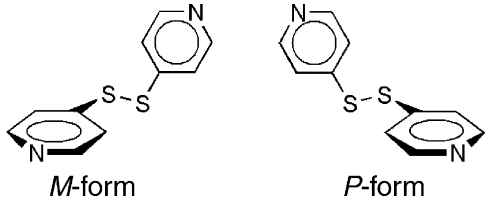

Fig. 4. Enantiomers of 4DPDS.

metric disulfide derivatives undergo disproportion in solution to give symmetric disulfide compounds. Accordingly, it is difficult to isolate 1:1 or 1:2 M:L molecular complexes containing asymmetrically coordinated 4DPDS (Fig. 5), a feature that might facilitate high-yield production of the coordination polymers. Furthermore, cleavage of the S–S bond allows an efficient means of introducing spacers into 4DPDS. For example, 4,6-bis(4′-pyridylsulfide)dibenzofuran [30] and bis(thiopyridyl)ferrocenes [31,32] (Fig. 1) are obtained by treatment of the corresponding lithiated spacers with 4DPDS. This is an attractive route to functional ligands.

4DPDS behaves as a bidentate N-donor ligand, but the bridging sulfur atoms can have additional coordination ability. 2,2′-Dipyridyldisulfide (2DPDS), an isomer of 4DPDS, coordinates to metal ions in an N,S- or N,N-chelate fashion to produce molecular complexes (Fig. 6) [33], and 4,4′-dipyridylsulfide (4DPS; Fig. 1) can coordinate to a Ag(I) ion at the thioether moiety, producing high-dimensional coordination polymers [34]. However, coordination at the thioether moiety has not been observed for 4DPDS even when combined with soft metal ions, such as Ag(I).

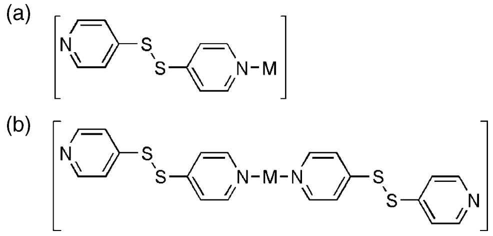

Fig. 5. Examples of 4DPDS molecular complexes that are not isolable. (a) 1:1 M:L complex and (b) 1:2 M:L complex.

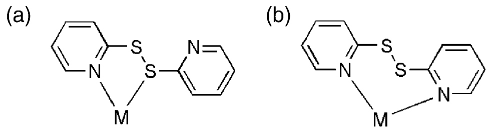

Fig. 6. (a) N,S-chelate and (b) N,N-chelate coordination modes of 2DPDS.

Comparison with alkyl-bridged ligands reveals the characteristics of the S–S bond. 1,2-Bis(4-pyridyl)ethane (4BPEa; Fig. 1), which is structurally related to 4DPDS, is a flexible ligand with two conformers with respect to the twist angle: *anti* and *gauche*. In contrast, the disulfide moiety in 4DPDS is rigid and does not adopt an *anti* conformation. The torsion angles of C–S–S–C in complexes of 4DPDS range from 78.0° to 96.5° (average 87.6°; Table 1). Despite the rigidity of the S–S bridging group in 4DPDS, its coordination polymers show various structures when assembled, as discussed in the following sections.

3. Synthesis and structures of metal complexes with 4DPDS

3.1. Macrocycle structures

4DPDS generates 2:2 M:L macrocyclic compounds, which can be achiral or chiral with *cis*-metal salts (Fig. 7). The achiral macrocycle contains two 4DPDS ligands of different chirality, while the chiral form contains two ligands with the same chirality. The macrocyclic units are chiral in most cases, but they form racemic crystals and no chiral crystals have been discovered.

The complexes accommodate counter-anions or small solvent molecules above and below the macrocycles, though the

Table 1
C—S—S—C torsion angles and cavity sizes in 4DPDS coordination complexes

Compound	Topology	C—S—S—C torsion angle (°)	Cavity size (Å^2)	Reference
$[\{Pt(PEt_3)_2(4DPDS)\}_2(NO_3)_4]$ (**1**)	Macrocycle	91.7	95.7[a]	[35]
$[\{Ir(H)_2(PPh_3)_2(4DPDS)\}_2(BF_4)_2 \cdot (CH_2Cl_2)_3 \cdot H_2O]$ (**2**)	Macrocycle	87.4, 87.2	100.6[a]	[36]
$[\{Co(hfac)_2(4DPDS)\}_2 \cdot (CHCl_3)_4]$ (**3**)	Macrocycle	90.8, 89.1	98.3[a]	[37]
$[\{Ni(hfac)_2(4DPDS)\}_2 \cdot (CHCl_3)_4]$ (**4**)	Macrocycle	91.3, 89.5	98.3[a]	[37]
$[\{Co(hfac)_2(4DPDS)\}_2 \cdot H_2O]$ (**5**)	Macrocycle	78.5	98.9[a]	[37]
$[\{Ni(hfac)_2(4DPDS)\}_2 \cdot H_2O]$ (**6**)	Macrocycle	78.0	98.0[a]	[37]
$[Mn(hfac)_2(4DPDS)]_n$ (**7**)	Zigzag chain	90.9	–	[40]
$[Mn(hfac)_2(4DPDS)]_n$ (**8**)	Helical chain	90.1	–	[37]
$[Cu(hfac)_2(4DPDS)]_n$ (**9**)	Helical chain	90.0	–	[40]
$[Ag(OTs)(4DPDS)]_n$ (**10**)	Zigzag chain	96.2	–	[46]
$[\{Ag(4DPDS)\}NO_3 \cdot (CH_3CN)_{0.5}]_n$ (**11**)	Helical chain	83.2	–	[46]
$[\{Cu(C_6H_5COO)_2\}_2(4DPDS)]_n$ (**12**)	Zigzag chain	86.5	–	[50]
$[\{Cu(C_5H_{11}COO)_2\}_2(4DPDS)]_n$ (**13**)	Zigzag chain	90.6	–	[50]
$[Cu_4(CH_3COO)_6(\mu^3\text{-}OH)_2(4DPDS)_2]_n$ (**14**)	Ruffled ribbon	83.2, 81.3	59.9[b]	[50]
$[\{Cu(CH_3COO)_2(4DPDS)\} \cdot (H_2O)_6]_n$ (**15**)	Zigzag chain	96.5	134.6[c]	[50]
$[Zn_7(CH_3COO)_{10}(\mu^4\text{-}O)_2(4DPDS)]_n$ (**16**)	Zigzag chain	85.5	–	[52]
$[Zn(NCS)_2(4DPDS)]_n$ (**17**)	Chiral zigzag chain	91.2	–	[54]
$[\{Cd(H_2O)_2(4DPDS)_2\}(NO_3)_2 \cdot (C_2H_5OH)_2 \cdot (H_2O)_2]_n$ (**18**)	Repeated rhomboid	89.7	105.5[a]	[55]
$[\{Zn(NCS)_2(4DPDS)_2\} \cdot (DMF)_2]_n$ (**19**)	Repeated rhomboid	86.3	101.8[a]	[58]
$[\{Zn(H_2O)_2(4DPDS)_2\}(NO_3)_2 \cdot H_2O \cdot CH_3OH]_n$ (**20**)	Repeated rhomboid	91.1	100.3[a]	[58]
$[Zn(NO_3)_2(4DPDS)_2]_n$ (**21**)	Repeated rhomboid	87.2, 87.2	100.3[a]	[58]
$[\{Zn(NO_3)(H_2O)(4DPDS)_2\}NO_3 \cdot (H_2O)_4]_n$ (**22**)	Repeated rhomboid	88.9, 88.9	100.6[a]	[58]
$[\{Zn(DMSO)_2(4DPDS)_2\}(ClO_4)_2]_n$ (**23**)	Repeated rhomboid	88.8	100.4[a]	[58]
$[\{Zn(H_2O)_2(4DPDS)_2\}(ClO_4)_2 \cdot (4DPDS)_4]_n$ (**24**)	Repeated rhomboid	90.3, 85.9 (arm)	101.4[a]	[58]
$[\{Cu(H_2O)(4DPDS)_2\}(NO_3)_2 \cdot (H_2O)_3]_n$ (**25**)	Repeated rhomboid	89.7	96.6[a]	[64]
$[\{Cu(SO_4)(4DPDS)_2\} \cdot (H_2O)_{1.5} \cdot CH_3OH]_n$ (**26**)	Repeated rhomboid	88.4	104.7[a]	[64]
$[\{Fe(NCS)_2(4DPDS)_2\} \cdot (H_2O)_4]_n$ (**27**)	Repeated rhomboid	80.9	101.5[a]	[54]
$[\{Co(4DPDS)_2\}(Cl)_2 \cdot (CH_3OH)_2]_n$ (**28**)	Repeated rhomboid	91.5	97.9[a]	[54]
$[CuI(4DPDS) \cdot (CH_3CN)]_n$ (**29**)	Planar ribbon	83.6	124.0[d]	[65]
$[CuI(4DPDS) \cdot (CH_2Cl_2)]_n$ (**30**)	Planar ribbon	85.7	125.2[d]	[65]
$[\{(CuI)_2(4DPDS)\}_2 \cdot (CH_3CH_2CN)]_n$ (**31**)	Necklace chain	77.4	120.9[d]	[65]
$[\{(CuI)_2(4DPDS)\}_2 \cdot (CH_3CN)]_n$ (**32**)	Tubular chain	79.5	123.8[d]	[65]
$[CdCl_2(4DPDS)_2]_n$ (**33**)	Sheet	90.5	–	[64]
$[\{Ag(4DPDS)_2\}PF_6]_n$ (**34**)	Sheet	91.4	–	[46]
$[\{Ag(4DPDS)_2\}ClO_4]_n$ (**35**)	Sheet	89.7	–	[46]

[a] Estimated by intramolecular M· · ·M and (S—S)· · ·(S—S) separations.
[b] Estimated by pyridine (centroid)· · ·pyridine (centroid) separations.
[c] Estimated by intramolecular Cu· · ·Cu separations.
[d] Estimated by intramolecular (Cu–Cu)· · ·(Cu–Cu) and (S—S)· · ·(S—S) separations.

cavities are too small to encapsulate larger organic molecules. The cavity sizes, measured by intramolecular M· · ·M separations (10.1–11.0 Å) and (S–S)· · ·(S–S) separations (8.7–9.7 Å), are approximately 100 Å^2 (Table 1), being almost independent of metal species, counter-anions and guest molecules.

Stang and co-workers have prepared a discrete macrocyclic compound $[\{Pt(PEt_3)_2(4DPDS)\}_2(NO_3)_4]$ (**1**) by using 4DPDS and *cis*-$Pt(PEt_3)_2(NO_3)_2$ [35]. The macrocycle comprises two 4DPDS ligands of different chirality and two *cis*-platinum salts, and exhibits a chair-like structure (Fig. 8). To the best of our

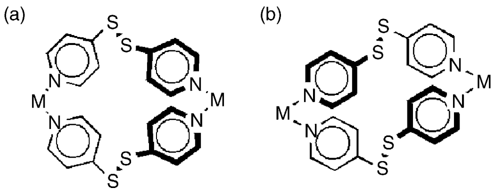

Fig. 7. Schematic illustrations of (a) achiral and (b) chiral 4DPDS macrocycles.

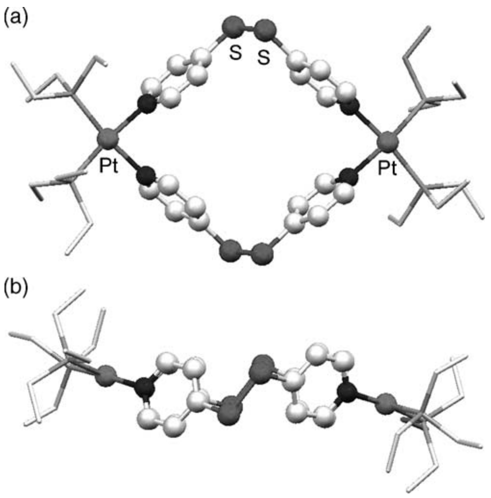

Fig. 8. Macrocycle structure of **1**: (a) top view and (b) side view. Counter-anions are omitted for clarity.

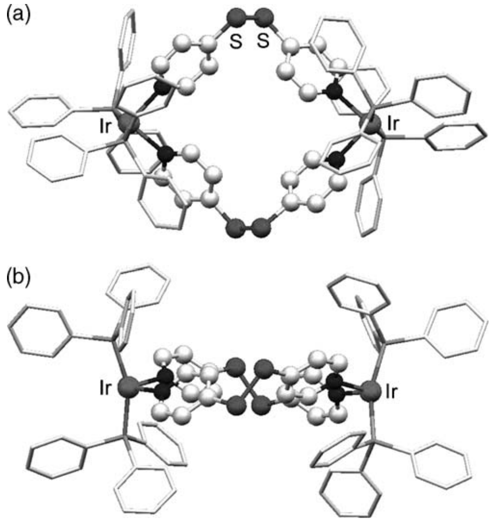

Fig. 9. Macrocycle structure of **2**: (a) top view and (b) side view. Solvent molecules are omitted for clarity.

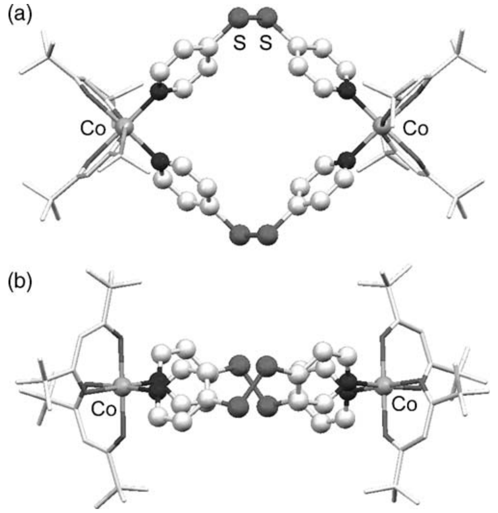

Fig. 10. Macrocycle structure of **3**: (a) top view and (b) side view. Solvent molecules are omitted for clarity.

knowledge, this compound is the only example of an achiral 4DPDS macrocyclic complex. The nitrate anions of **1** fit above and below the macrocycle, and the cavity size is somewhat smaller than chiral macrocycles (Table 1) because of its chair-like structure. This compound does not incorporate solvent molecules in the crystal lattice.

An iridium hydrido complex [{Ir(H)$_2$(PPh$_3$)$_2$(4DPDS)}$_2$ (BF$_4$)$_2$·(CH$_2$Cl$_2$)$_3$·H$_2$O] (**2**) has been prepared by Maekawa and co-workers [36]. This complex has a chiral macrocyclic structure that consists of two 4DPDS ligands with the same chirality (Fig. 9). The iridium ion adopts a slightly distorted octahedral coordination geometry with two *cis* pyridyl nitrogens. Two tetrafluoroborate anions occupy sites above and below the macrocycle. Guest solvent molecules occupy the interstices between the macrocycles.

The reaction of 4DPDS with M(hfac)$_2$(H$_2$O)$_2$ (M = Co, Ni; hfac = 1,1,1,5,5,5-hexafluoroacetylacetonate) in a mixture of chloroform and diethyl ether produces [{M(hfac)$_2$(4DPDS)}$_2$·(CHCl$_3$)$_4$] [M = Co (**3**), Ni (**4**)] [37]. Assembled structures adopted by 4DPDS complexes with M(hfac)$_2$ are summarized in Scheme 1. Complexes **3** and **4** are isomorphous and involve two *cis* M(hfac)$_2$ units as shown in Fig. 10. These complexes accommodate four solvent chloroform molecules in intermolecular interstices; two of which occupy sites above and below the

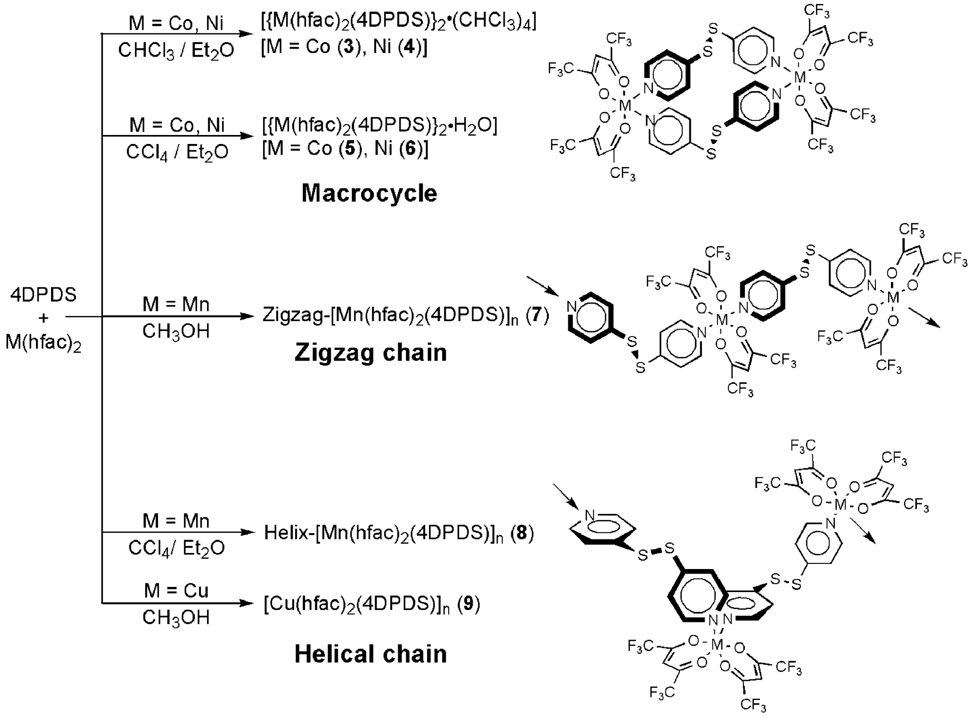

Scheme 1. Structural classification of 4DPDS complexes with M(hfac)$_2$.

macrocycle, and the other two are outside the macrocycle. Complexes **3** and **4** easily release their solvent molecules to give non-crystalline solids, which are no longer soluble in common organic solvents.

[{M(hfac)$_2$(4DPDS)}$_2$·H$_2$O] [M = Co (**5**), Ni (**6**)] can be obtained from the combination of 4DPDS and corresponding metal salts in a solution of tetrachloromethane and diethyl ether (Scheme 1) [37]. These compounds are isomorphous, and although their molecular structures are very similar to those of **3** and **4**, the packing arrangements are different: the packing of **5** and **6** is solvent-dependent. In contrast to **3**, the guest molecules in **5** are located outside the macrocycle, and the sites above and below the macrocycle are occupied by the tetrafluoromethane moiety of adjacent macrocycles. In contrast to **3** and **4**, dried samples of **5** and **6** are slightly soluble in common organic solvents, which indicates that the macrocyclic structures are retained after loss of solvent. When **5** is recrystallized from tetrachloromethane or chlorobenzene, solvent inclusion compounds (**5**·CCl$_4$ and **5**·PhCl) are obtained.

3.2. One-dimensional structures

The most extensively studied coordination polymers are one-dimensional. 4DPDS affords one-dimensional coordination polymers with zigzag, helical and repeated rhomboidal structures.

3.2.1. Zigzag and helical chains

One-dimensional chains with 1:1 M:L stoichiometry can be classified into two groups: zigzag and helical. The zigzag chain is achiral in most cases, being constructed from alternating links of metal ion and 4DPDS with the *M*- and *P*-forms. Only one complex with a chiral zigzag chain structure is known. The helical chain is chiral, containing ligands with the same chirality. However, no chiral crystals have been isolated; all known crystals involve a 1:1 ratio of *M*- and *P*-chains, crystallized in an achiral space group.

3.2.1.1. M(hfac)$_2$ complexes. The two vacant sites of M(hfac)$_2$ facilitate the construction of low-dimensional coordination polymers using bidentate ligands [31,38,39]. Combination of 4DPDS with *cis*-M(hfac)$_2$ produces either the 2:2 M:L macrocycles described above or 1:1 M:L helical chains, while use of *trans*-M(hfac)$_2$ leads to 1:1 M:L one-dimensional chains.

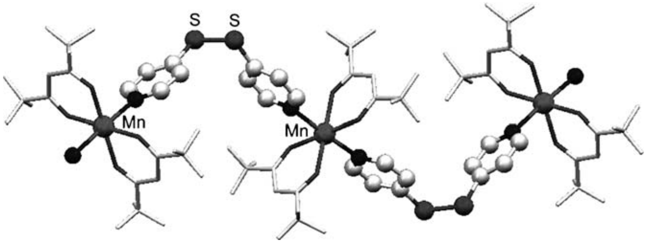

Fig. 11. Zigzag chain structure of **7**.

The structure of the manganese compound [Mn(hfac)$_2$(4DPDS)]$_n$ is solvent-dependent. A zigzag chain complex, zigzag-[Mn(hfac)$_2$(4DPDS)]$_n$ (**7**), can be obtained by the reaction of Mn(hfac)$_2$(H$_2$O)$_2$ and 4DPDS in methanol or chloroform (Scheme 1) [40]. The structure of **7** is depicted in Fig. 11 and is composed of achiral chains in which the ligands occupy the *trans* positions of the manganese ion. Interestingly, the same reaction in a mixture of tetrachloromethane and diethyl ether produces helix-[Mn(hfac)$_2$(4DPDS)]$_n$ (**8**), in which Mn(hfac)$_2$ adopts the *cis* configuration to produce chiral chains (Fig. 12) [37]. Such a solvent effect is rare, and some related phenomena are described in Section 3.2.3. Thus, choice of solvent is crucial for the manganese complex; however, the structure of the analogous copper complex [Cu(hfac)$_2$(4DPDS)]$_n$ (**9**) is independent of reaction solvent [40], being isomorphous to helix-[Mn(hfac)$_2$(4DPDS)]$_n$ (**8**).

A difference between 4DPDS and related ligands can be seen in the M···M separations. The nearest intra-chain M···M separations in **7** and **8** are ca. 10.3 and 11.5 Å, respectively, which are shorter than those found in [Mn(hfac)$_2$(4BPEe)]$_n$ (4BPEe = 1,2-bis(4-pyridyl)ethylene; Fig. 1) (ca. 13.9 Å) [41] and [Cu(hfac)$_2$(4BPEa)]$_n$ (ca. 13.3 Å) [38]. Owing to the bent structure of 4DPDS, the lone pairs of the pyridine rings are nearly perpendicular, while those in ethane- or ethylene-bridged ligands are nearly parallel. This leads to the shorter intra-chain M···M separations in 4DPDS complexes (Fig. 13).

3.2.1.2. Silver(I) complexes. The Ag(I) ion can adopt various coordination geometries, including linear, T-shaped and tetrahedral [18,42], so coordination polymers with Ag(I) salts differ widely. For example, when Ag(I) salts are combined with 4BPY, the resultant structures can be one- or two-dimensional [43–45]. Similarly, structures of Ag(I)–4DPDS complexes vary depending on the coordination geometry of the metal ion: linear and

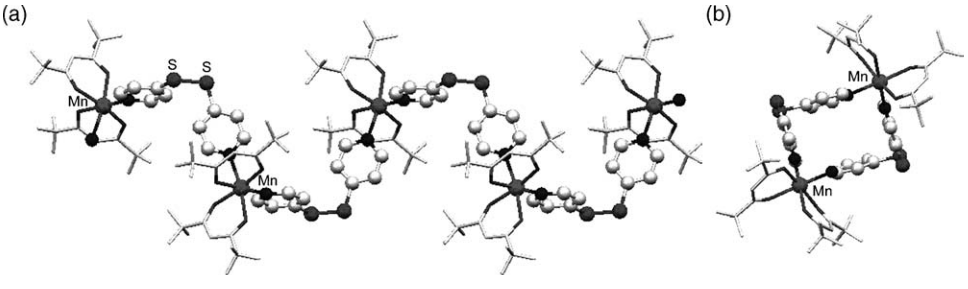

Fig. 12. Helical chain structure of **8** viewed along (a) the *a*-axis and (b) the *c*-axis.

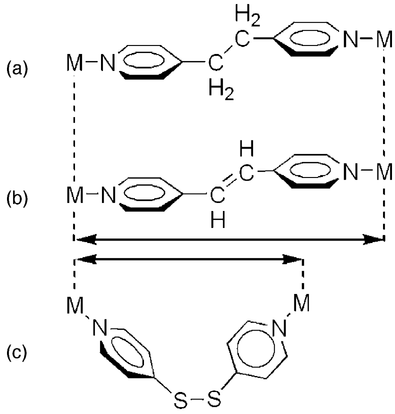

Fig. 13. M···M separations in complexes with (a) 4BPEa, (b) 4BPEe and (c) 4DPDS.

T-shaped coordination geometries lead to a one-dimensional chain, while a tetrahedral geometry results in a two-dimensional sheet (Scheme 2).

[Ag(OTs)(4DPDS)]$_n$ (OTs = *p*-toluenesulfonate) (**10**) and [{Ag(4DPDS)}NO$_3$·(CH$_3$CN)$_{0.5}$]$_n$ (**11**) both form 1:1 M:L one-

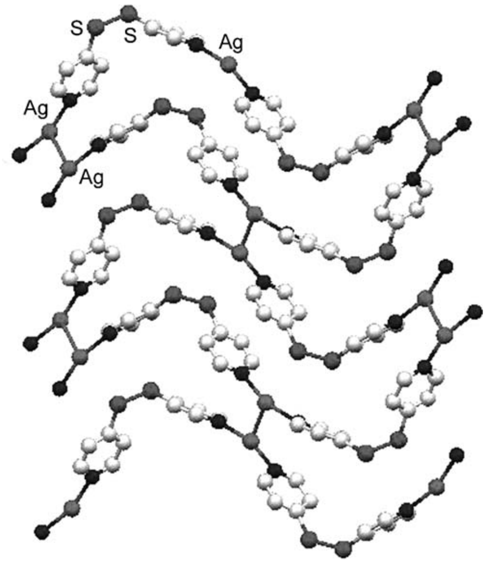

Fig. 14. Zigzag chain structure of **10**. Counter-anions are omitted for clarity.

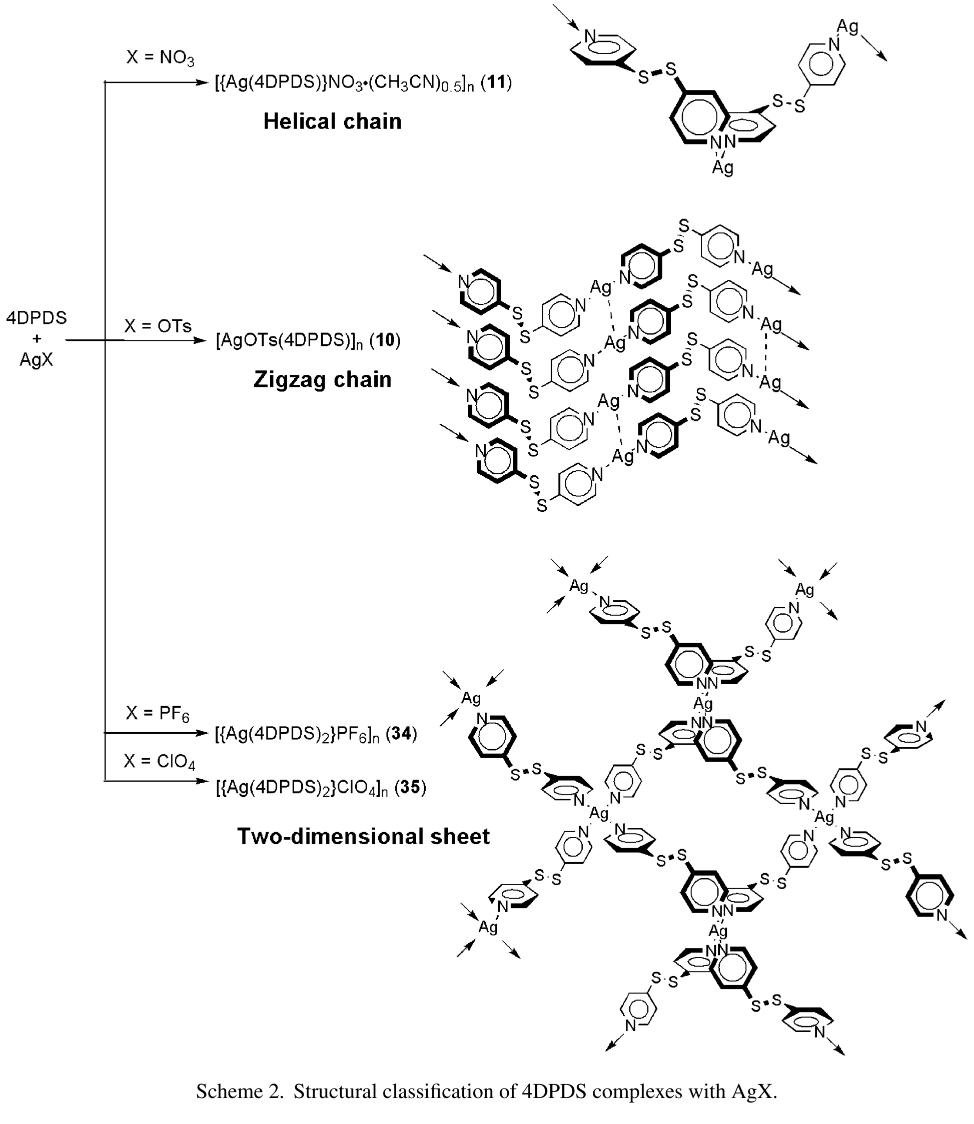

Scheme 2. Structural classification of 4DPDS complexes with AgX.

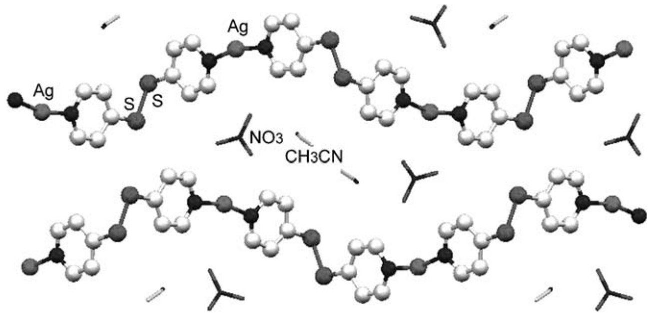

Fig. 15. Helical chain structure of **11**.

dimensional chains [46], but their assembled structures differ as shown in Figs. 14 and 15, respectively. Although the local structure of **10** is an achiral chain, the structure overall is a pseudo-two-dimensional sheet where chains are bridged by inter-chain Ag···Ag interactions (3.044(2) Å). The OTs counter-anions are located between sheets. In contrast, compound **11** shows a chiral chain structure with guest acetonitrile molecules incorporated between the chains.

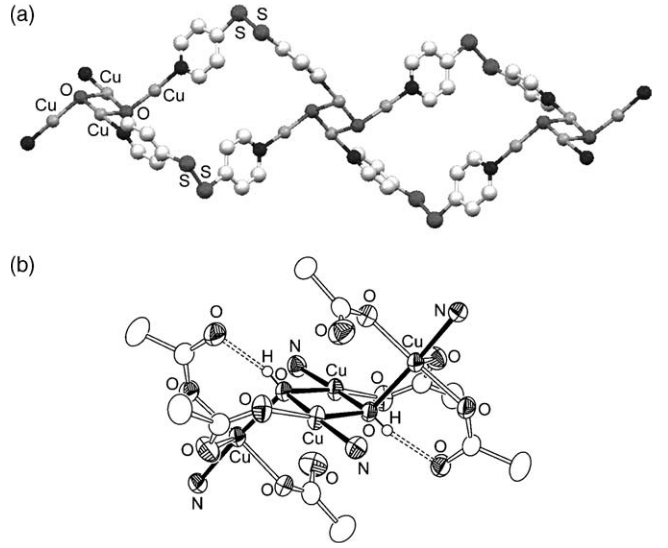

Fig. 17. (a) Repeated rhomboidal structure of **14**. Counter-anions are omitted for clarity. (b) ORTEP drawing around the $[Cu_4(CH_3COO)_4(OH)_2]$ core in **14**. Dashed lines indicate hydrogen bonds.

3.2.1.3. Copper(II) and zinc(II) carboxylate complexes. The copper(II) carboxylates provide various polynuclear structures including the “paddlewheel” lantern-like dinuclear unit [47–49].

Fig. 16 shows the zigzag chain structure of $[\{Cu(C_6H_5COO)_2\}_2(4DPDS)]_n$ (**12**), in which the paddlewheel $[Cu(C_6H_5COO)_2]_2$ units are linked by 4DPDS [50]. The structure of $[\{Cu(C_5H_{11}COO)_2\}_2(4DPDS)]_n$ (**13**) is very similar. Crystals of **12** contain two crystallographically independent paddlewheel units that have almost identical structures. However, the reaction of $[\{Cu(CH_3COO)_2\}_2 \cdot H_2O]$ with 4DPDS produces a 4:2 M:L coordination polymer $[Cu_4(CH_3COO)_6(\mu_3\text{-}OH)_2(4DPDS)_2]_n$ (**14**), as shown in Fig. 17 [50]. The hydroxo groups are from the water molecules; **14** does not form under anhydrous conditions. The structure of **14** consists of alternating links of a $Cu_4(CH_3COO)_6(\mu_3\text{-}OH)_2$ butterfly core and two 4DPDS ligands with opposite chirality, making a ruffled ribbon structure (Figs. 17a and 3b). The cavity area is ca. 60 Å^2 (Table 1), which is much smaller than those of macrocycles **1–6** (∼100 Å^2). This difference is a result of cavity shape: that of **14** is ruffled, while macrocycles **1–6** have rhomboidal cavities. In the butterfly core, two hydroxo oxygen atoms link three Cu(II) ions in a μ_3 fashion to construct two $Cu_3O(H)$ tetrahedra, which share a Cu···Cu edge. Further, intramolecular hydrogen bonds connect the hydroxo hydrogen and the carboxylato oxygen, as indicated by dashed lines in Fig. 17b. The structure of the Cu(II) tetranuclear core is reflected in its magnetic susceptibility: the Cu(II) ions have antiferromagnetic interactions via the two hydroxo oxygen atoms.

The structures of these 4DPDS complexes indicate that copper carboxylates with large substituents (C_6H_5–, C_5H_{11}–) maintain the dinuclear paddlewheel structures, but those with a small substituent (CH_3–) do not. An analogous phenomenon is observed in the Cu(II) carboxylate complexes with 4-aminopyridine: the copper hexanate complex $[Cu(C_5H_{11}COO)_2(4\text{-aminopyridine})_2]$ shows a mononuclear structure, while the copper acetate complex $[Cu_4(CH_3COO)_6(\mu_3\text{-}OH)_2(4\text{-aminopyridine})_4]$ has a tetranuclear structure similar to the butterfly core of **14** [51].

Interestingly, the 4:2 M:L compound **14** can be transformed into a 1:1 M:L coordination polymer $[\{Cu(CH_3COO)_2(4DPDS)\} \cdot (H_2O)_6]_n$ (**15**) by recrystallization from aqueous solution [50]. This conversion is accompanied by a change in crystal color and shape: compounds **14** and **15** crystallize as blue-green blocks and sky-blue plates, respectively. The Cu(II) ion in **15** adopts square-planar geometry, coordinated by two pyridine nitrogens and two carboxylate oxygen atoms. Its assembled structure shows a honeycomb-like network (Fig. 18) formed by the assembly of one-dimensional helical chains. There are two helical chains in **15**, running approximately perpendicular to each other, along the *a* and *c*–*b* directions, respectively. The honeycomb channels are occupied by counter anions and guest water molecules, and the size of the open channel is estimated by intra-chain M···M separations to be ca. 12 Å × 12 Å. At room temperature, this compound gradually releases the guest molecules and decomposes. The number of water molecules present has been determined by elemental analysis and thermogravimetric analysis, but their precise positions in the channel have not been crystallographically determined.

The reaction of zinc acetate and 4DPDS affords a 7:1 M:L zigzag chain $[Zn_7(CH_3COO)_{10}(\mu_4\text{-}O)_2(4DPDS)]_n$ (**16**) [52].

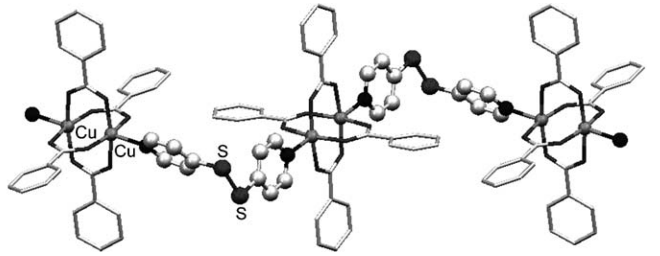

Fig. 16. Zigzag chain structure of **12**.

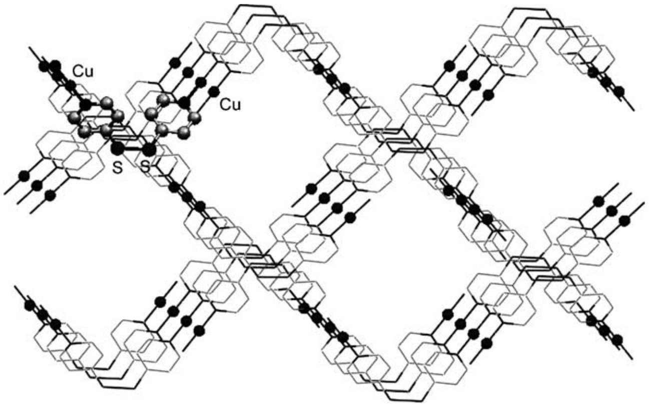

Fig. 18. Honeycomb structure of **15**. Counter-anions and guest molecules are omitted for clarity.

The heptanuclear zinc clusters are linked by 4DPDS, as shown in Fig. 19. The Zn(II) ion that resides at the center of the cluster possesses an octahedral coordination geometry, while the others adopt a highly distorted tetrahedral geometry. The Zn(II) ions are connected by carboxylate anions and two oxygen atoms. The overall structure of **16** is different from that of the related compound $[Zn_7(CH_3COO)_{10}(\mu_4\text{-}O)_2(4BPEa)]_n$, which is a linear coordination polymer [52]. This difference is associated with the shape of the different ligand; 4BPEa can adopt an *anti*-conformation and provide straight-chain coordination polymers.

3.2.1.4. Zinc(II) complex. The Zn(II) ion is often employed to construct coordination polymers because it can adopt a tetrahedral coordination geometry, which can lead to high dimensional networks [6,53]. Besides, the ion shows no significant d–d transition in the visible region, which is advantageous for NLO materials [53].

$[Zn(NCS)_2(4DPDS)]_n$ (**17**) can be obtained by the reaction of zinc(II) nitrate, ammonium thiocyanate and 4DPDS in methanol [54]. This is the only example of a chiral complex with a zigzag chain structure. The metal ion adopts a tetrahedral geometry, linked by the 4DPDS ligands with the same chirality (Fig. 20). Interchain S···S contacts are found between the thiocyanate group and 4DPDS (3.64 Å), which is shorter than the van der Waals distance (3.7 Å).

3.2.2. Repeated rhomboids

The repeated rhomboid structures (Fig. 21) are composed of an equatorial coordinated metal ion and two bent bridging ligands. The local structure can be regarded as similar to that of the macrocycles, and, accordingly, repeated rhomboids with 4DPDS also show chiral or achiral structures. Furthermore, as observed for the macrocycles, the guest molecules or counter anions occupy sites above and below the rhomboids. Their guest-inclusion abilities are more efficient than the macrocycles. The repeated rhomboids are in most cases stacked face-to-face, constructing crystal packings that resemble the pillared-layer structure, which further promotes guest-inclusion properties. Among other ligands, *gauche*-4BPEa [36] and 4DPS [25,55] also provide the repeated rhomboid structures, but few such structures are known for linear bridging ligands.

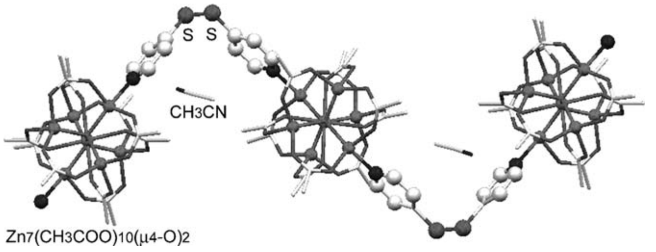

Fig. 19. Zigzag chain structure of **16**.

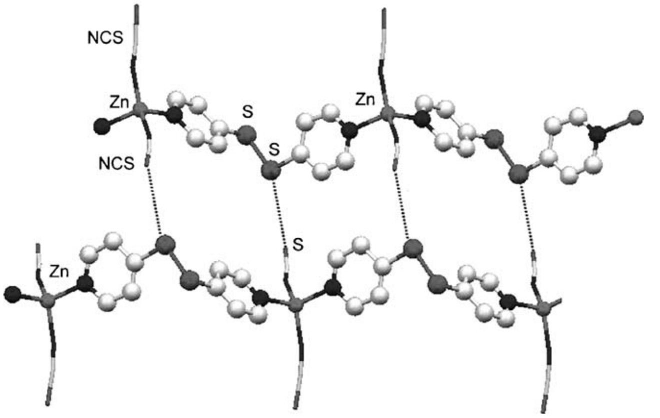

Fig. 20. Chiral zigzag chain structure of **17**. Dashed lines indicate S···S interactions.

3.2.2.1. Cadmium(II) and zinc(II) complexes. The d^{10} electron configurations of Cd(II) and Zn(II) allow a variety of coordination geometries, similar to the Ag(I) ion [53,56].

A Cd(II) compound, $[\{Cd(H_2O)_2(4DPDS)_2\}(NO_3)_2\cdot(C_2H_5OH)_2\cdot(H_2O)_2]_n$ (**18**), can be obtained by the combination of 4DPDS with $Cd(NO_3)_2$ [57]. The polymeric structure consists of repeated achiral rhomboids (Fig. 22). The repeated rhomboid chains stack face-to-face to form channels (cavity area: 106 Å^2) (Fig. 22). The Cd(II) ions adopt an octahedral coordination geometry and are coordinated by four pyridine nitrogen atoms and two water oxygen atoms. The guest molecules and nitrate anions are located between the repeated rhomboidal chains, and form hydrogen bonds with the coordinated water molecules.

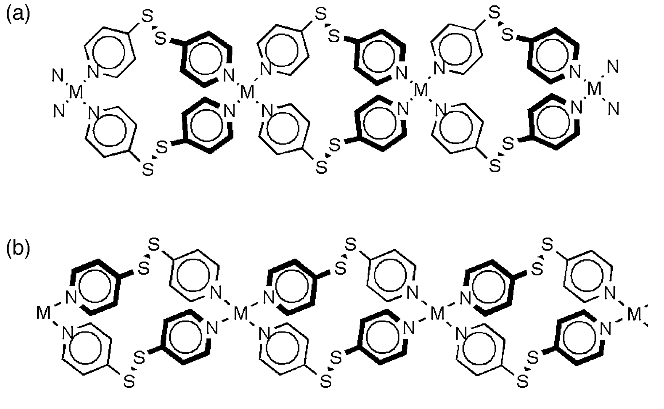

Fig. 21. Schematic illustrations of (a) achiral and (b) chiral repeated rhomboidal chains from 4DPDS.

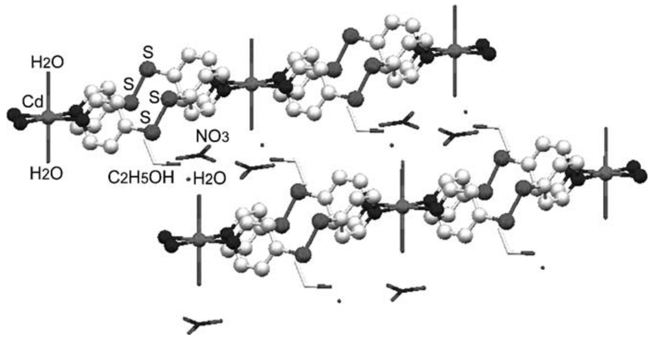

Fig. 22. Achiral repeated rhomboid structure of **18**.

Compound **18** retains crystallinity after removal of the guest molecules by vacuum drying, but the crystal structure is altered and the dried material is unable to absorb gas, unlike porous coordination polymers.

As shown in Scheme 3, the reactions of 4DPDS with ZnX_2 (X = SCN, NO_3, ClO_4) produce 1:2 M:L complexes with repeated rhomboids, $[\{ZnL^1L^2(4DPDS)_2\}A{\cdot}G]_n$, where L is a ligand in the apical position, A an uncoordinated counter-anion and G a guest molecule. These complexes enclathrate various guest molecules: $L^1 = L^2 = NCS$, A = none, G = $(DMF)_2$ (**19**); $L^1 = L^2 = H_2O$, A = $(NO_3)_2$, G = $H_2O{\cdot}CH_3OH$ (**20**); $L^1 = L^2 = NO_3$, A = none, G = none (**21**); $L^1 = NO_3$, $L^2 = H_2O$, A = NO_3, G = $(H_2O)_4$ (**22**); $L^1 = L^2 = DMSO$, A = $(ClO_4)_2$, G = none (**23**); $L^1 = L^2 = H_2O$, A = $(ClO_4)_2$, G = $(4DPDS)_4$ (**24**) [58]. These complexes are obtained from recrystallization of the corresponding precursor complex $[ZnX_2(4DPDS)_2{\cdot}(solvent)]$. Except for **19**, the structures of all these complexes are solvent-dependent. Despite the various coordination geometries available to Zn(II) ions, the 4DPDS complexes contain only six-coordinated zinc octahedra.

The thiocyanate derivative $[Zn(NCS)_2(4DPDS){\cdot}(DMF)_2]_n$ (**19**) has an achiral repeated-rhomboid structure, constructed from alternate links of a Zn(II) ion and two enantiomers of 4DPDS, while $[Zn(NCS)_2(4DPDS)]_n$ (**17**), involving no guest molecule, has a chiral zigzag structure (vide supra). The complex accommodates DMF molecules above and below each rhomboid. There is no significant interaction between the rhomboid and the guest DMF molecules, so the latter are gradually released. The nitrate derivative **20**, obtained by recrystallization from a methanol solution of the precursor complex, also has an achiral structure. Compound **20** incorporates two coordination water molecules, a guest water and a guest methanol. The methanol molecules lie above and below the rhomboid, while the water molecule is located outside the rhomboid. The nitrate anion and the coordination water form hydrogen bonds with the guest molecules.

The two chiral nitrate derivatives **21** and **22** are obtained by recrystallization of the precursor complex from DMF and aqueous solutions, respectively; their structures are depicted in Figs. 23 and 24. In each case, the stacked rhomboidal chains are slightly shifted with respect to adjacent chains, so the rhomboids do not form channels. In **21,** the nitrate anions that coordinate to the Zn(II) in the adjacent rhomboids are located above and below the rhomboid, and this complex enclathrates no sol-

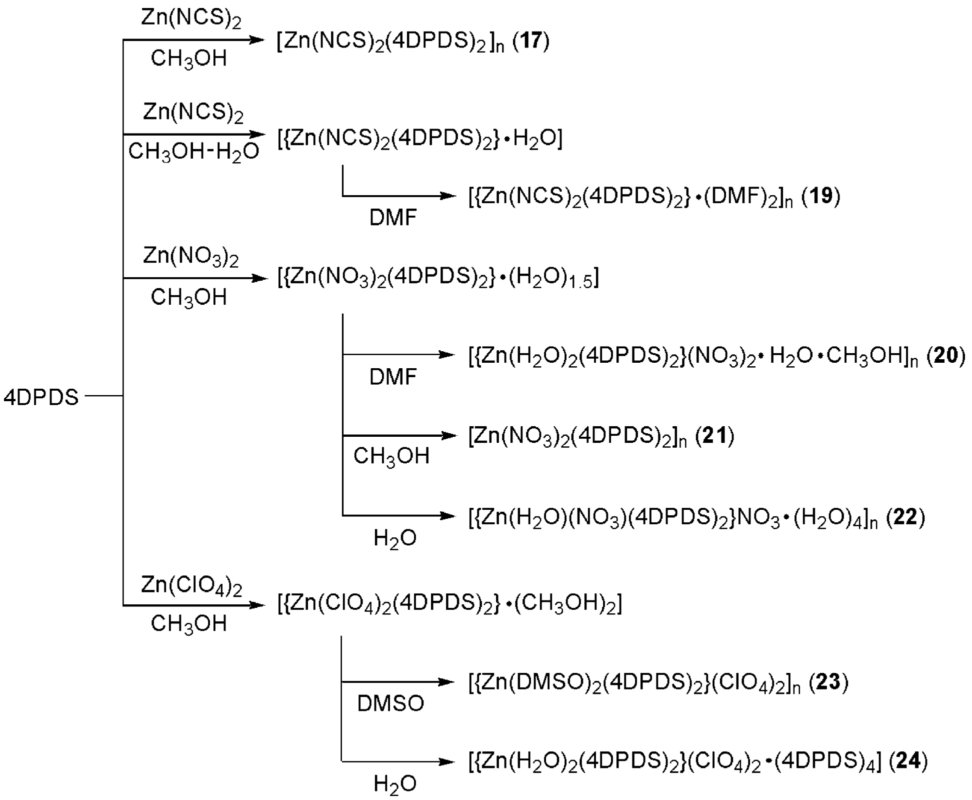

Scheme 3. Solvent dependence of the reaction products of 4DPDS with ZnX_2.

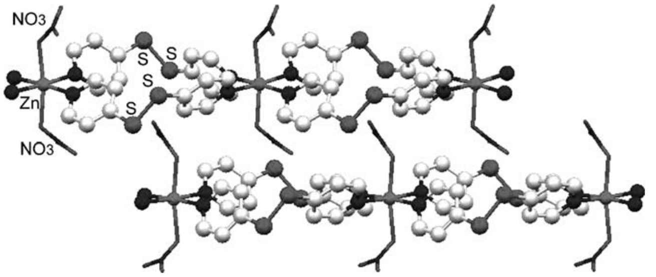

Fig. 23. Chiral repeated rhomboid structure of **21**.

vent molecules. In contrast, **22** includes a coordination water molecule and four solvent water molecules, which form hydrogen bonds with the nitrate anions to construct a pseudo-three-dimensional network structure (Fig. 24b). This network can be regarded as a pillared-layer structure.

The perchlorate complexes **23** and **24** are obtained by recrystallization of the precursor complex from DMSO and water, respectively; their chiral repeated rhomboid structures are shown in Figs. 25 and 26, respectively. Compound **23**, which has a 1:1 ratio of chains with opposite chirality**,** has a non-centrosymmetric space group (*P*-4). This compound has two crossed channels, parallel to the *a* and *b* axes, respectively. The axial positions of the Zn(II) ion in **23** are coordinated by two DMSO molecules, while those in **24** are occupied by two water molecules. The coordinated water molecules form hydrogen bonds with two free 4DPDS molecules, constructing an armed repeated rhomboid structure. The 4DPDS arms do not link the repeated rhomboid chains, and the free pyridine moieties are located above and below adjacent rhomboids.

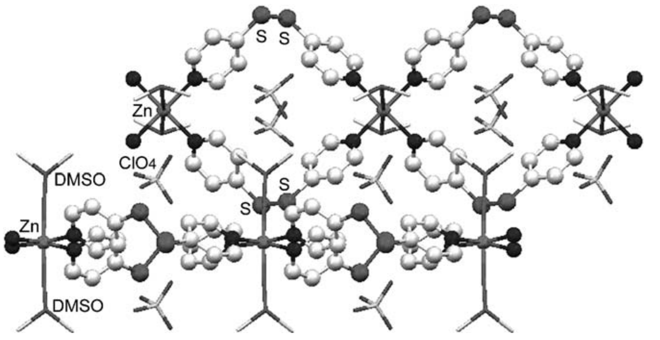

Fig. 25. Chiral repeated rhomboid structure of **23** viewed along the *b*-axis.

3.2.2.2. Copper(II), iron(II) and cobalt(II) complexes. Due to their diverse coordination geometries and magnetic properties,

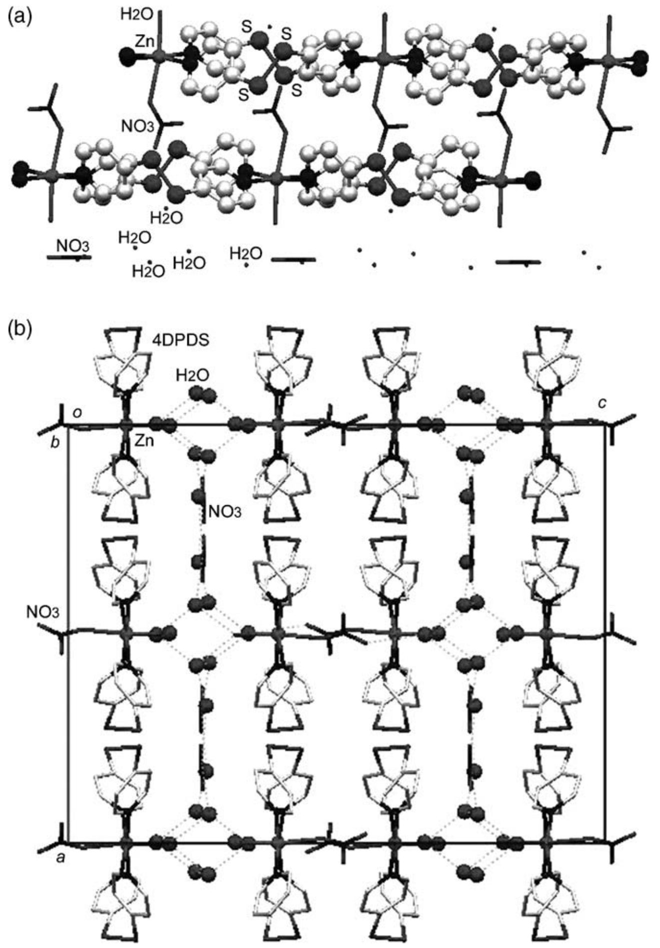

Fig. 24. (a) Chiral repeated rhomboid structure of **22**. (b) Pseudo-three-dimensional network structure of **22**. Dashed lines indicate hydrogen bonds.

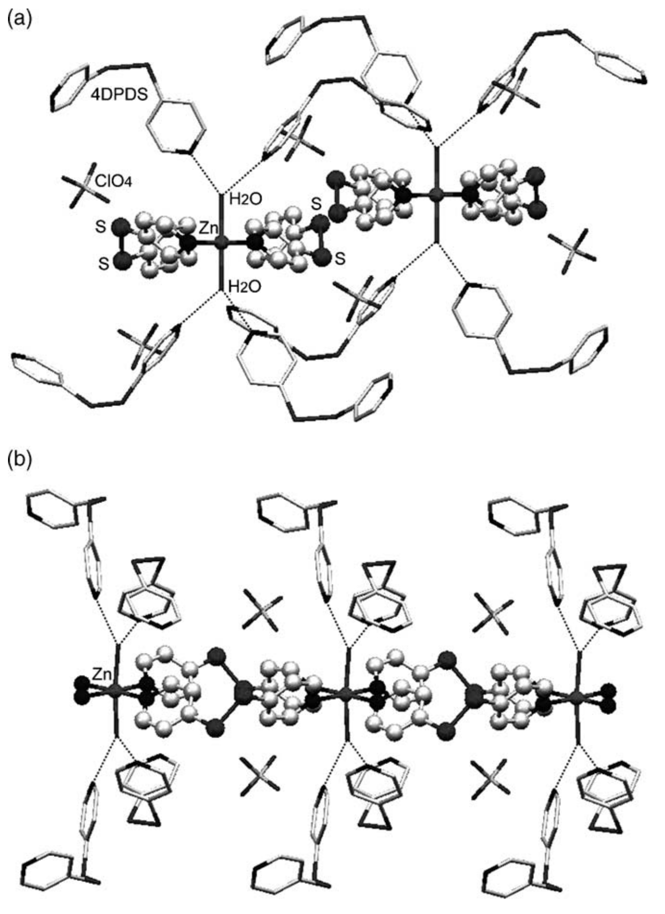

Fig. 26. Chiral repeated rhomboid structure of **24** with hydrogen-bonded 4DPDS arms viewed along (a) the *b*-axis and (b) the *c*-axis. Dashed lines indicate hydrogen bonds.

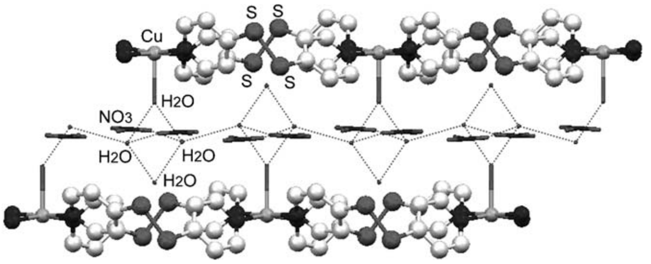

Fig. 27. Repeated rhomboid chain of **25**, linked via hydrogen bonds to form a double chain structure. Dashed lines indicate hydrogen bonds.

Cu(II), Fe(II) and Co(II) salts are often employed to build functional coordination polymers [38,59–63].

Two Cu(II) derivatives $[\{Cu(H_2O)(4DPDS)_2\}(NO_3)_2\cdot(H_2O)_3]_n$ (**25**) and $[\{Cu(SO_4)(4DPDS)_2\}\cdot(H_2O)_{1.5}\cdot CH_3OH]_n$ (**26**) have the chiral repeated rhomboid structure, as shown in Figs. 27 and 28, respectively [64]. In **25**, the repeated rhomboids are linked via hydrogen bonds between the coordination water molecules, the nitrate anion and the guest water molecules, to form double chains. Complex **26** shows a two-dimensional sheet structure in which the one-dimensional repeated rhomboids are bridged by coordinating sulfate anions. In this compound, the water molecules are located between the sheets while the methanol molecules are located above and below the rhomboids. Although the local structure in each complex is chiral, the overall structures are achiral because they contain chains with both chiralities. As for magnetic properties, **25** shows an antiferromagnetic intra-chain interaction between the Cu(II) ions, while the Cu(II) ions of **26** have an intra-chain antiferromagnetic interaction and an inter-chain ferromagnetic interaction.

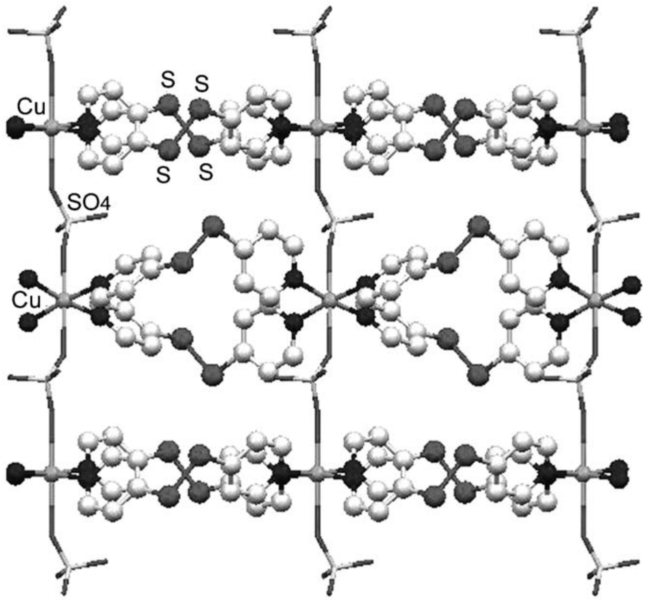

Fig. 28. Two-dimensional sheet structure of **26**. Solvent molecules are omitted for clarity.

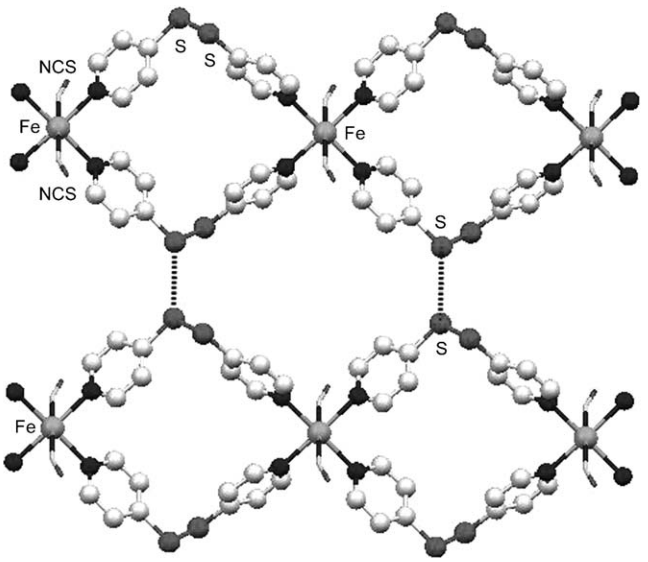

Fig. 29. Repeated rhomboid chain of **27**. Solvent molecules are omitted for clarity. Dashed lines indicate S· · ·S interactions.

An Fe(II) complex $[\{Fe(NCS)_2(4DPDS)_2\}\cdot(H_2O)_4]_n$ (**27**) is formed by the reaction of iron(II) sulfate, 4DPDS and ammonium thiocyanate [54]. The structure consists of repeated chiral rhomboids (Fig. 29). The axial thiocyanato anions of the adjacent rhomboids are located above and below the rhomboids, while the guest water molecules occupy the interstices between the repeated rhomboids. The inter-chain $S_{4DPDS}\cdots S_{4DPDS}$ distance is 3.52 Å (Fig. 29), indicating the presence of significant S· · ·S interactions. This type of complex should be interesting from the viewpoint of spin-crossover [63].

The reaction of cobalt(II) chloride with 4DPDS affords a chiral repeated rhomboid complex $[\{Co(4DPDS)_2\}(Cl)_2\cdot(CH_3OH)_2]_n$ (**28**) [54]. The structure contains alternate links of a square-planar Co(II) ion and two 4DPDS molecules with the same chirality. The chloride anions are located at the axial positions of the metal center with a long Co· · ·Cl distance (2.916 Å).

3.2.3. Supramolecular isomerism (topological isomerism)

Choice of reaction solvent is often crucial in the formation of coordination polymers, because it can govern yields and product structures. The solvent can act as a guest, as a ligand and as a template for the supramolecule. Moulton and Zaworotko have demonstrated that the Co(II) compound $[Co(NO_3)_2(4BPEa)_{1.5}]_n$ shows two different structures, associated with the different conformations of the ligand, and they referred to this phenomenon as “supramolecular isomerism” [4,62]. The relationship between zigzag-$[Mn(hfac)_2(4DPDS)]_n$ (**7**) and helix-$[Mn(hfac)_2(4DPDS)]_n$ (**8**) corresponds to this type of isomerism (Scheme 1).

An interesting study of the supramolecular isomerism of one-dimensional coordination polymers of copper(I) iodide with 4DPDS has been done by Blake et al. [65]. Copper(I) halides produce square dimer, cubane tetramer and stair polymeric structures, which provide interesting coordination chemistry [39,49,66,67]. They isolated four one-dimensional coordination polymers: $[CuI(4DPDS)\cdot(guest)]_n$ [guest = CH_3CN (**29**); CH_2Cl_2 (**30**)] and $[\{(CuI)_2(4DPDS)\}_2\cdot(guest)]_n$ [guest = CH_3CH_2CN (**31**); CH_3CN (**32**)]. Slow diffusion of an

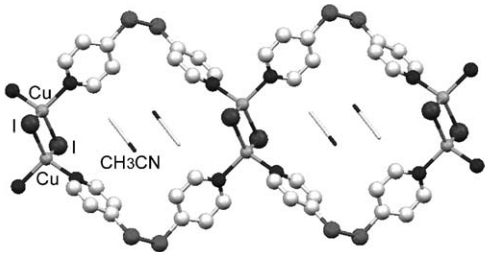

Fig. 30. Planar ribbon structure of **29**.

acetonitrile solution of CuI into a dichloromethane solution of 4DPDS produces the 1:1 M:L complex **29** in the ligand-rich (lower) layer and the 2:1 M:L complex **31** in the metal-rich (upper) layer. Similarly, complexes **30** and **32** can be obtained in the ligand-rich and metal-rich regions, respectively, by using cyanoethane instead of acetonitrile. Compounds **29** and **30** have similar planar ribbon structures, while the structures of **31** and **32** are necklace-like and tubular, respectively (Fig. 3b).

The planar ribbons **29** and **30** comprise Cu_2I_2 rhomboidal cores linked by two 4DPDS molecules (Fig. 30). The compounds incorporate acetonitrile and dichloromethane molecules, respectively, as guests between the ribbons. Interestingly, **29** accommodates the CuI solvent while **30** accommodates the solvent of 4DPDS, despite similar synthetic procedures. The necklace structure of **31** is constructed from alternate links of macrocycles composed of a Cu_4I_4 cubane core and two 4DPDS ligands. Adjacent macrocycles are perpendicular and enclathrate CH_3CH_2CN molecules, as shown in Fig. 31. The structure of **32** is quite different; two zigzag chains consisting of alternate links of 4DPDS and Cu_4I_4 tetrahedra are linked by two 4DPDS ligands (Fig. 32). The packing structure of **32** involves two crossed channels that run parallel to the *a* and *b* axes and accommodate acetonitrile molecules.

The structural differences between **31** and **32** may be attributed to a solvent template effect. These examples demonstrate how the structures and compositions of the coordination polymers with 4DPDS depend on reaction conditions.

3.3. Two-dimensional structures

Examples of two-dimensional coordination polymers with 4DPDS are fewer than those with other bis-pyridine-type ligands. This is probably owing to the twisted structure of the ligand. As described above, the reaction solvent may act as a template for the assembled structures. Similarly, the counteranion plays an important role.

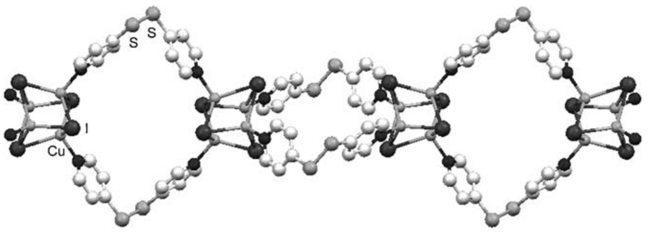

Fig. 31. Necklace-like structure of **31**. Solvent molecules are omitted for clarity.

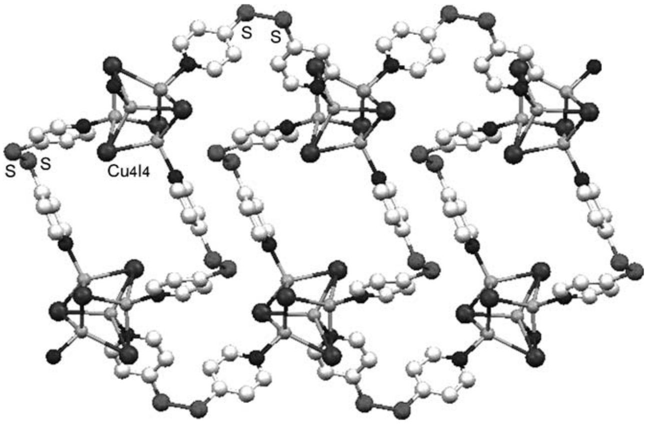

Fig. 32. Tubular structure of **32**. Solvent molecules are omitted for clarity.

Combination of cadmium(II) chloride with 4DPDS generates a two-dimensional sheet complex $[CdCl_2(4DPDS)_2]_n$ (**33**) with a puckered rhombus grid structure (Fig. 33) [64]. The Cd(II) ion in **33** adopts an octahedral geometry, the equatorial positions being occupied by the nitrogen atoms of 4DPDS. Although the coordination environments around the Cd(II) ion are similar in **18** and **33**, the overall structures are different. **18** has a one-dimensional repeated rhomboid structure, while the sheets in **33** are tightly packed. Complex **33** accommodates no guest molecules, unlike **18**. Each sheet in **33** is achiral, containing both enantiomers of 4DPDS. Complex **33** exhibits a weak broad emission at around 350–500 nm and a sharp emission at 575 nm ($\lambda_{ex} = 314$ nm) at room temperature in the solid state. These emissions are attributed to an inter-ligand transition and a ligand-to-metal charge-transfer transition, respectively.

$[\{Ag(4DPDS)_2\}PF_6]_n$ (**34**) has a two-dimensional sheet structure, the local structure of which resembles the Möbius strip (Fig. 34) [46]. The ring is constructed from four approximately

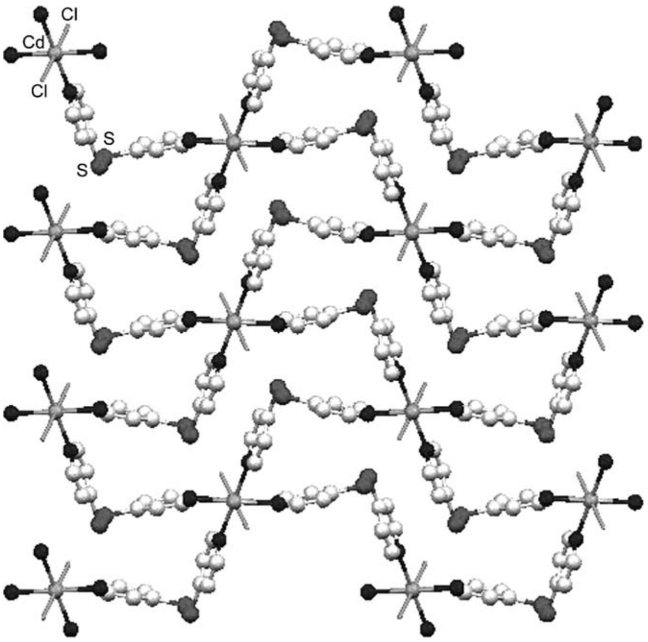

Fig. 33. Two-dimensional sheet structure of **33**.

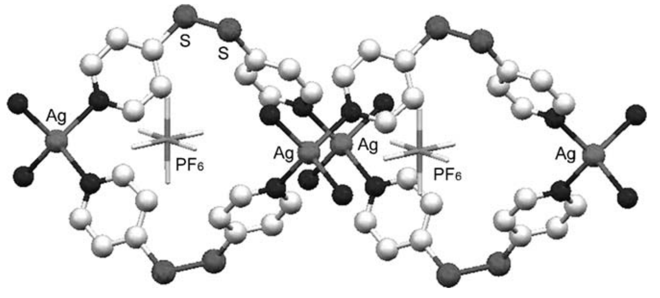

Fig. 34. Möbius-strip-like structure of **34**.

tetrahedral Ag(I) ions coordinated by four nitrogen atoms from four 4DPDS ligands, and surrounds two hexafluorophosphate anions, which, we speculate, act as a template for assembly. The Ag(I) perchlorate complex $[\{Ag(4DPDS)_2\}ClO_4]_n$ (**35**) is isomorphous to **34**, and these complexes do not enclathrate guest molecules [46]. Interestingly, each Möbius strip consists of only *P*- or *M*-4DPDS; therefore, the two-dimensional sheet is chiral. However, the crystal has a centrosymmetric space group and contains sheets of opposite chirality.

Acknowledgments

The authors thank Grant-in-Aid for Scientific Research (No. 17685003) from Japan Society for the Promotion of Science (JSPS) and the “High-Tech Research Center” Project 2005–2009 from Ministry of Education, Culture, Sports, Science and Technology (MEXT) for financial support.

References

[1] J.-M. Lehn, Supramolecular Chemistry, Concepts and Perspectives, VCH, Weinheim, 1995.
[2] J.-M. Lehn, J.L. Atwood, J.E.D. Davis, D.D. MacNicol, F. Vögtle (Eds.), Comprehensive Supramolecular Chemistry, Pergamon Press, Oxford, 1990–1996, p. 1.
[3] Coord. Chem. Rev. 246 (2003) (Special issue of Structure, properties and application of inorganic polymers, and references cited therein).
[4] B. Moulton, M.J. Zaworotko, Chem. Rev. 101 (2001) 1629.
[5] C.V.K. Sharma, J. Chem. Educ. 78 (2001) 617.
[6] N.R. Champness, J. Chem. Soc., Dalton Trans. (2006) 877.
[7] J.L. Atwood, L.J. Barbour, Cryst. Growth Des. 3 (2003) 3.
[8] L. Brammer, Chem. Soc. Rev. 33 (2004) 476.
[9] C. Janiak, J. Chem. Soc., Dalton Trans. (2003) 2781.
[10] O. Kahn, Acc. Chem. Res. 33 (2000) 647.
[11] M.J. Zaworotko, Chem. Commun. (2001) 1.
[12] P.J. Hagrman, D. Hagrman, J. Zubieta, Angew. Chem. Int. Ed. 38 (1999) 2638.
[13] G.F. Swiegers, T.J. Malefetse, Coord. Chem. Rev. 225 (2002) 91.
[14] S.R. Seidel, P.J. Stang, Acc. Chem. Res. 35 (2002) 972.
[15] For example. D.B. Cordes, A.S. Bailey, P.L. Caradoc-Davies, D.H. Gregory, L.R. Hanton, K. Lee, M.D. Spicer, Inorg. Chem. 44 (2005) 2544.
[16] M. Fujita, Chem. Soc. Rev. 27 (1998) 417.
[17] B. Olenyuk, A. Fechtenkötter, P.J. Stang, J. Chem. Soc., Dalton Trans. (1998) 1707.
[18] M.J. Plater, M.R.St.J. Foreman, T. Gelbrich, S.J. Coles, M.B. Hursthouse, J. Chem. Soc., Dalton Trans. (2000) 3065.
[19] Y.-B. Dong, J.-P. Ma, R.-Q. Huang, M.D. Smith, H.-C. zur Loye, Inorg. Chem. 42 (2003) 294.
[20] L. Carlucci, G. Ciani, D.W.v. Gudenberg, D.M. Proserpio, Inorg. Chem. 36 (1997) 3812.
[21] M.J. Plater, M.R.St.J. Foreman, T. Gelbrich, M.B. Hursthouse, Inorg. Chim. Acta 318 (2001) 171.
[22] H. Hou, Y. Song, Y. Fan, L. Zhang, C. Du, Y. Zhu, Inorg. Chim. Acta 316 (2001) 140.
[23] M.C. Laskoski, R.L. LaDuca Jr., R.S. Rarig Jr., J. Zubieta, J. Chem. Soc., Dalton Trans. (1999) 3467.
[24] D.M.L. Goodgame, D.A. Grachvogel, S. Holland, N.J. Long, A.J.P. White, D.J. Williams, J. Chem. Soc., Dalton Trans. (1999) 3473.
[25] O.-K. Jung, S.H. Park, D.C. Kim, K.M. Kim, Inorg. Chem. 37 (1998) 610.
[26] C.M. Drain, J.-M. Lehn, J. Chem. Soc., Chem. Commun. (1994) 2313.
[27] L. Carlucci, G. Ciani, D.M. Proserpio, J. Chem. Soc., Dalton Trans. (1999) 1799.
[28] B.-L. Fei, W.-Y. Sun, K.-B. Yu, W.-X. Tang, J. Chem. Soc., Dalton Trans. (2000) 805.
[29] J.A.R. Navarro, B. Lippert, Coord. Chem. Rev. 222 (2001) 219.
[30] P.L. Caradoc-Davies, L.R. Hanton, J. Chem. Soc., Dalton Trans. (2003) 1754.
[31] R. Horikoshi, T. Mochida, H. Moriyama, Inorg. Chem. 41 (2002) 3017.
[32] R. Horikoshi, T. Mochida, R. Torigoe, Y. Yamamoto, Eur. J. Inorg. Chem. (2002) 3197.
[33] M.M. Kadooka, L.G. Warner, K. Seff, J. Am. Chem. Soc. 98 (1976) 7569.
[34] O.-S. Jung, S.H. Park, C.H. Park, J.K. Park, Chem. Lett. 27 (1999) 923.
[35] F.M. Tabellion, S.R. Seidel, A.M. Arif, P.J. Stang, J. Am. Chem. Soc. 123 (2001) 7740.
[36] X.-Y. Yu, M. Maekawa, T. Morita, H.-C. Chang, S. Kitagawa, G.-X. Jin, Bull. Chem. Soc. Jpn. 75 (2002) 267.
[37] R. Horikoshi, T. Mochida, M. Kurihara, M. Mikuriya, Cryst. Growth Des. 5 (2005) 243.
[38] Y.-B. Dong, M.D. Smith, R.C. Layland, H.-C. zur Loye, Inorg. Chem. 38 (1999) 5027.
[39] R. Horikoshi, M. Ueda, T. Mochida, New J. Chem. 26 (2002) 933.
[40] R. Horikoshi, T. Mochida, H. Moriyama, Inorg. Chem. 40 (2001) 2430.
[41] G. Mago, M. Hinago, H. Miyasaka, N. Matsumoto, H. Okawa, Inorg. Chim. Acta 254 (1997) 145.
[42] D. Venkataraman, S. Lee, J.S. Moore, P. Zhang, K.A. Hirsch, G.B. Gardner, A.C. Covey, C.L. Prentice, Chem. Mater. 8 (1996) 2030.
[43] M.L. Tong, X.-M. Chen, S.W. Ng, Inorg. Chem. Commun. 3 (2000) 436.
[44] O.M. Yaghi, H. Li, J. Am. Chem. Soc. 118 (1996) 295.
[45] F. Robinson, M.J. Zaworotko, J. Chem. Soc., Chem. Commun. (1995) 2413.
[46] R. Horikoshi, T. Mochida, N. Maki, S. Yamada, H. Moriyama, J. Chem. Soc., Dalton Trans. (2002) 28.
[47] M. Mikuriya, H. Azuma, M. Handa, Mol. Cryst. Liq. Cryst. 379 (2002) 205.
[48] R. Horikoshi, K. Okazawa, T. Mochida, J. Organomet. Chem. 690 (2005) 1793.
[49] T. Mochida, K. Okazawa, R. Horikoshi, J. Chem. Soc., Dalton Trans. (2006) 693.
[50] R. Horikoshi, M. Mikuriya, Bull. Chem. Soc. Jpn. 78 (2005) 827.
[51] N. Lah, J. Koller, G. Giester, P. Segedin, I. Leban, New J. Chem. 26 (2002) 933.
[52] M.T. Ng, T.C. Deivaraj, J.J. Vittal, Inorg. Chim. Acta 348 (2003) 173.
[53] O.R. Evans, W. Lin, Acc. Chem. Res. 35 (2002) 511.
[54] M.-C. Suen, Y.-H. Wang, Y.-F. Hsu, C.-W. Yeh, J.-D. Chen, J.-C. Wang, Polyhedron 24 (2005) 2913.
[55] M. Kondo, Y. Shimizu, M. Miyazawa, Y. Irie, A. Nakamura, T. Naito, K. Maeda, F. Uchida, T. Nakamoto, A. Inaba, Chem. Lett. 33 (2004) 514.
[56] A. Erxleben, Coord. Chem. Rev. 246 (2003) 203.
[57] M. Kondo, M. Shimamura, S. Noro, Y. Kimura, K. Uemura, S. Kitagawa, J. Solid State Chem. 152 (2000) 113.
[58] R. Horikoshi, M. Mikuriya, Cryst. Growth Des. 5 (2005) 223.
[59] K. Adachi, Y. Sugiyama, H. Kumagai, K. Ionue, S. Kitagawa, S. Kawata, Polyhedron 20 (2001) 1411.

[60] M.-L. Tong, H.-J. Chen, X.-M. Chen, Inorg. Chem. 39 (2000) 2235.
[61] J.Y. Lu, A.M. Babb, Inorg. Chem. 40 (2001) 3261.
[62] H. Gudbjartson, K. Biradha, K.M. Poirier, M.J. Zaworotko, J. Am. Chem. Soc. 121 (1999) 2599.
[63] J.A. Real, E. Andrés, M.C. Muñoz, M. Julve, T. Granier, A. Bousseksou, F. Varret, Science 268 (1995) 265.
[64] J. Luo, M. Hong, R. Wang, D. Yuan, R. Cao, L. Han, Y. Xu, Z. Lin, Eur. J. Inorg. Chem. (2003) 3623.
[65] A.J. Blake, N.R. Brook, N.R. Champness, M. Crew, A. Deveson, D. Fenske, D.H. Gregory, L.R. Hanton, P. Hubberstey, M. Schröder, Chem. Commun. (2001) 1432.
[66] P.M. Graham, R.D. Pike, M. Sabat, R.D. Bailey, W.T. Pennington, Inorg. Chem. 39 (2000) 5121.
[67] A.J. Blake, N.R. Brook, N.R. Champness, L.R. Hanton, P. Hubberstey, M. Schröder, Pure Appl. Chem. 70 (1998) 2351.